Locust density shapes energy metabolism and oxidative stress resulting in divergence of flight traits

Baozhen Du[a,b,1], Ding Ding[c,1], Chuan Ma[c], Wei Guo[b,c,2], and Le Kang[a,b,c,2]

[a]Beijing Institutes of Life Science, Chinese Academy of Sciences, Beijing 100101, China; [b]Center for Excellence in Biotic Interactions, University of Chinese Academy of Sciences, Beijing 100049, China; and [c]State Key Laboratory of Integrated Management of Pest Insects and Rodents, Institute of Zoology, Chinese Academy of Sciences, Beijing 100101, China

Contributed by Le Kang; received August 26, 2021; accepted November 10, 2021; reviewed by David Denlinger and Jon Harrison

Flight ability is essential for the enormous diversity and evolutionary success of insects. The migratory locusts exhibit flight capacity plasticity in gregarious and solitary individuals closely linked with different density experiences. However, the differential mechanisms underlying flight traits of locusts are largely unexplored. Here, we investigated the variation of flight capacity by using behavioral, physiological, and multiomics approaches. Behavioral assays showed that solitary locusts possess high initial flight speeds and short-term flight, whereas gregarious locusts can fly for a longer distance at a relatively lower speed. Metabolome–transcriptome analysis revealed that solitary locusts have more active flight muscle energy metabolism than gregarious locusts, whereas gregarious locusts show less evidence of reactive oxygen species production during flight. The repression of metabolic activity by RNA interference markedly reduced the initial flight speed of solitary locusts. Elevating the oxidative stress by paraquat injection remarkably inhibited the long-distance flight of gregarious locusts. In respective crowding and isolation treatments, energy metabolic profiles and flight traits of solitary and gregarious locusts were reversed, indicating that the differentiation of flight capacity depended on density and can be reshaped rapidly. The density-dependent flight traits of locusts were attributed to the plasticity of energy metabolism and degree of oxidative stress production but not energy storage. The findings provided insights into the mechanism underlying the trade-off between velocity and sustainability in animal locomotion and movement.

animal flight | energy metabolism | oxidative stress | long-distance migration

Insect flight capacity depends on several factors, such as wing morphology, hormone regulation, and energy metabolism (1). Plastic changes in wing morphology have been intensively studied in wing-dimorphic insects (2–4). Juvenile hormone, ecdysteroids, and insulin or insulin-like growth factor signaling pathways contribute to wing dimorphism regulation (5–7). Unlike wing-dimorphic insects, wing-monomorphic insects can transform their flight capacity within one generation (8). A central challenge in studying wing-monomorphic insect flight is understanding how insects regulate energy metabolism for a long-distance flight given their small body size and relatively short life span (9). Animal flight is among the physical activities with the highest energy consumption. During flight, the metabolic rate (MR) is at least 50 times that in normal physical activities (10, 11). A link between fuel energy metabolism and dispersal ability has been suggested in some butterfly species, i.e., the degree of dispersal increases with the MR (12, 13). However, the relationship between flight MR and flight capacity remains controversial.

Locusts are the most dangerous agricultural pests in the world. The migratory locust (*Locusta migratoria*) is a typical wing monomorphic insect that exhibits reversible phase changes between solitary and gregarious forms in response to population density variation (14, 15). The morphology, physiology, and behavioral traits of gregarious locusts at high population density remarkably differ from those of conspecific solitary locusts at a low population density (16–18). With increasing population density, gregarious locusts can form extremely dense hopper bands or migratory adult swarms, inflicting considerable damage within a short time. Moreover, gregarious adults can fly continuously for ∼12 h, causing plague outbreaks in remote regions. By contrast, solitary adults possess limited performance in long-distance flight, and they fly only when looking for mates and food or escaping from predators (14). Differences in behavior, body color, immunity, metabolism, and reproduction between gregarious and solitary locusts have been increasingly elucidated over the years (16–18). As an excellent model system for insect-flight studies, the migratory locust has been extensively used to investigate the energetic mobilization and metabolic regulation of flight (19). Gregarious locusts have higher lipid reserves and higher hyperlipidemic responses to flight than solitary ones. The content of adipokinetic hormones (AKHs), a neuropeptide family that regulates energetic

Significance

Migratory locusts display striking phenotypical plasticity. Gregarious locusts at high density can migrate long distances and cause huge economic losses of crops. By contrast, solitary locusts at low density have limited ability in long-distance flight. However, the mechanisms underlying such flight capacity variation are poorly understood. Here, we found that the flight muscle of solitary locusts has a higher catabolic capacity that is associated with greater reactive oxygen species (ROS) generation during high-velocity flights. By contrast, a relatively lower catabolic capacity in gregarious locusts is associated with lower ROS generation during long-distance flights. This finding uncovers the metabolic mechanism of locust flight trait alteration in response to density changes and enhances our understanding of the biological processes enabling locust migration.

Author contributions: B.D. and L.K. designed research; B.D., W.G., and L.K. performed research; B.D., D.D., C.M., W.G., and L.K. analyzed data; and B.D., D.D., and L.K. wrote the paper.

Reviewers: D.D., The Ohio State University; and J.H., Arizona State University.

The authors declare no competing interest.

See online for related content such as Commentaries.

[1]B.D. and D.D. contributed equally to this work.

[2]To whom correspondence may be addressed. Email: guowei@ioz.ac.cn or lkang@ioz.ac.cn.

This article contains supporting information online at http://www.pnas.org/lookup/suppl/doi:10.1073/pnas.2115753118/-/DCSupplemental.

Published December 27, 2021.

mobilization during prolonged flight, is higher in the corpora cardiac of solitary locusts than that of gregarious locusts (20, 21). However, regulatory factors and mechanisms underlying the differentiation of flight capacity of gregarious and solitary locusts require further elucidation.

The development of multiomics technology provides powerful tools for studying insect behavior. For instance, comparative transcriptomic and genomic analyses have uncovered differences in gene expression between migratory and nonmigratory monarch butterflies or between the eastern and western populations of the monarch butterfly (22, 23). A combination of tethered flight tests and transcriptomic analyses has been used to determine transcriptional profile differences associated with flight activity in cotton bollworm (24). A genome-wide analysis of the migratory locust revealed the expansion of gene families involved in energy consumption and detoxification, thereby implying the genetic bases of long-distance flight capacities (25). Metabolome analysis can provide a "closer" glimpse into the phenotypic features of an organism and has been widely used to reveal the key components of insect biological processes (26). Therefore, a combination of metabolome and transcriptome analysis is a promising strategy to elucidate the metabolic mechanism of the flight capacity variation of solitary and gregarious locusts.

In the present study, we compared the flight traits and metabolomic and transcriptional profiles of solitary and gregarious locusts. Solitary locusts have high flight speeds with short flight durations. In contrast, gregarious locusts are capable of long-distance flight at relatively low speed. Metabolomic and transcriptomic analyses combined with functional studies revealed that the divergence of flight traits in solitary and gregarious locusts was due to their differences in energy metabolism and degree of oxidative stress production. The crowding and isolation of solitary and gregarious locusts reversed the metabolic profiles and behavioral traits, respectively. Thus, the flight trait differentiation of solitary and gregarious locusts was attributed to different population density experiences linked with varied energy metabolism and oxidative stress production.

Results

Solitary Locusts Possess Higher Flight Speed and Intermittent Flying, whereas Gregarious Locusts Exhibit Longer Flight Duration. To investigate the flight performance we selected the 14-d-old adult locusts for flight behavioral assay on computerized flight mills (27). Based on the mathematical model, four parameters of locusts, namely, maximum and average flight speed, flight distance, and flight duration, were recorded to reflect the flight performance. No significant differences in these parameters between males and females were observed after 1 h of flight test on the mills (*SI Appendix*, Fig. S1) regardless of locust phase status. To exclude the possible interference of reproduction on flight performance only male adults were used for further studies.

Morphological differences exist between gregarious and solitary locusts (Fig. 1*A*). Thus, we evaluated the effect of morphological traits on flight performance. Gregarious locusts had larger body weights than solitary ones (Fig. 1*B*), but no differences in wing length and wing width were observed (Fig. 1*C*). Correlation analyses confirmed that body weight had no significant correlation with maximum flight speed, average flight speed, flight duration, and flight distance, as shown in *SI Appendix*, Fig. S2.

To investigate the differences in flight performance between gregarious and solitary locusts we recorded the flight parameters at 0.25, 1, 2, 4, and 10 h of flight test. At the initial stage (0 to 0.25 h), solitary locusts displayed about 25% and 10% higher maximum (Fig. 1*D*) and average flight speeds (Fig. 1*E*), respectively, than gregarious locusts. However, the flight speed of solitary locusts dropped rapidly within 1 h and had no significant difference from that of gregarious locusts according to the results of prolonged flight tests (≥1 h) (Fig. 1*E*). Additionally, during prolonged flight tests (over 1 h), gregarious locusts exhibited better performance in terms of total flight distance and duration (Fig. 1 *F* and *G*), but solitary locusts showed a much longer total resting duration (Fig. 1 *H*). Based on average flight speed and flight muscle mass, flight kinetic energy was generated (28). Solitary locusts showed significantly higher flight muscle kinetic energy at time points within 0.25 h. During longer flight tests (over 0.25 h) there was no significant difference between gregarious and solitary locusts (Fig. 1*I*). In 10-h tests on flight mills, the average flight duration of gregarious locusts was ∼2.28 h. Some gregarious individuals were able to fly constantly for ∼8 h, with a flight distance of over 40 km. By contrast, the average flight duration of solitary locusts in the 10-h test was only ∼0.55 h, and the highest flight distance was no more than 5 km. Thus, solitary locusts flew at high speed only for a short time. Conversely, gregarious locusts were able to fly constantly at relatively low speed for a long time.

High Level of Energy Metabolism Confers High-Speed and Short-Term Flight to Solitary Locusts. To explore the molecular basis of flight trait differentiation we conducted the transcriptomic analysis of flight muscles in gregarious and solitary locusts. First, gene-expression profiles were compared when the insects were at rest conditions. A total of 741 differentially expressed genes (DEGs) were identified with $P < 0.01$. Approximately 451 of 741 DEGs were highly expressed in the flight muscles of solitary locusts and were enriched mostly in pathways involved in energy metabolism, including oxidative phosphorylation, carbon metabolism, tricarboxylic acid (TCA) cycle, glycolysis, fatty acid degradation, pyruvate metabolism, and fatty acid metabolism according to Kyoto Encyclopedia of Genes and Genomes (KEGG) signaling pathway analysis (adjusted $P < 0.01$, Fisher's exact test). However, the 290 DEGs highly expressed in gregarious locusts showed no significant enrichment in specific pathways (Fig. 2*A* and *SI Appendix*, Fig. S3). Therefore, the most obvious difference between gregarious and solitary locusts in flight muscles was energy metabolism.

To further authenticate the gene-expression profiles, DEGs were confirmed by real-time PCR (qRT-PCR). Consistent with transcriptome data (Fig. 2*B*), the transcription levels of genes involved in carbohydrate metabolism—phosphoglucomutase (*PGM*), hexokinase (*HK*), pyruvate kinase (*PYK*), glycogen phosphorylase (*GLY*), and fructose-bisphosphate aldolase (*ALDO*)—lipid metabolism—carnitine *O*-palmitoyltransferase1 (*CPT1*), carnitine *O*-palmitoyltransferase2 (*CPT2*), fatty acid binding protein (*FABP*), and very long-chain acyl-CoA dehydrogenase (*ACADVL*), TCA cycle, and oxidative phosphorylation—citrate synthase (*CS*), cytochrome *c* oxidase subunit4 (*COX4*), cytochrome *c* oxidase subunit7A (*COX7A*), adenosine 5′-triphosphate (ATP) synthase (*ATPsyn*), and NADH dehydrogenase subcomplex subunit (*NDUFA*)—were higher in solitary locusts than in gregarious ones (*SI Appendix*, Fig. S4). The activities of three rate-limiting enzymes HK, PYK, and CS were measured. In line with the gene-expression profiles, the activities of the enzymes were significantly higher in solitary locusts than in gregarious locusts (Fig. 2*C*). The levels of metabolites, acetyl-CoA and NADH, which were involved in mitochondrial aerobic metabolism, were higher in the flight muscles of solitary locusts (Fig. 2*D*). Similarly, the resting CO_2 production rate was significantly higher in solitary locusts (Fig. 2*E*). Thus, when at rest, solitary locusts are more active in energy metabolism than gregarious ones.

Next, the transcriptome and gene-expression profiles under flight conditions were tested. Transcriptomic analysis and qRT-PCR verification indicated that the energy metabolism gene expressions were significantly higher in solitary locusts than in

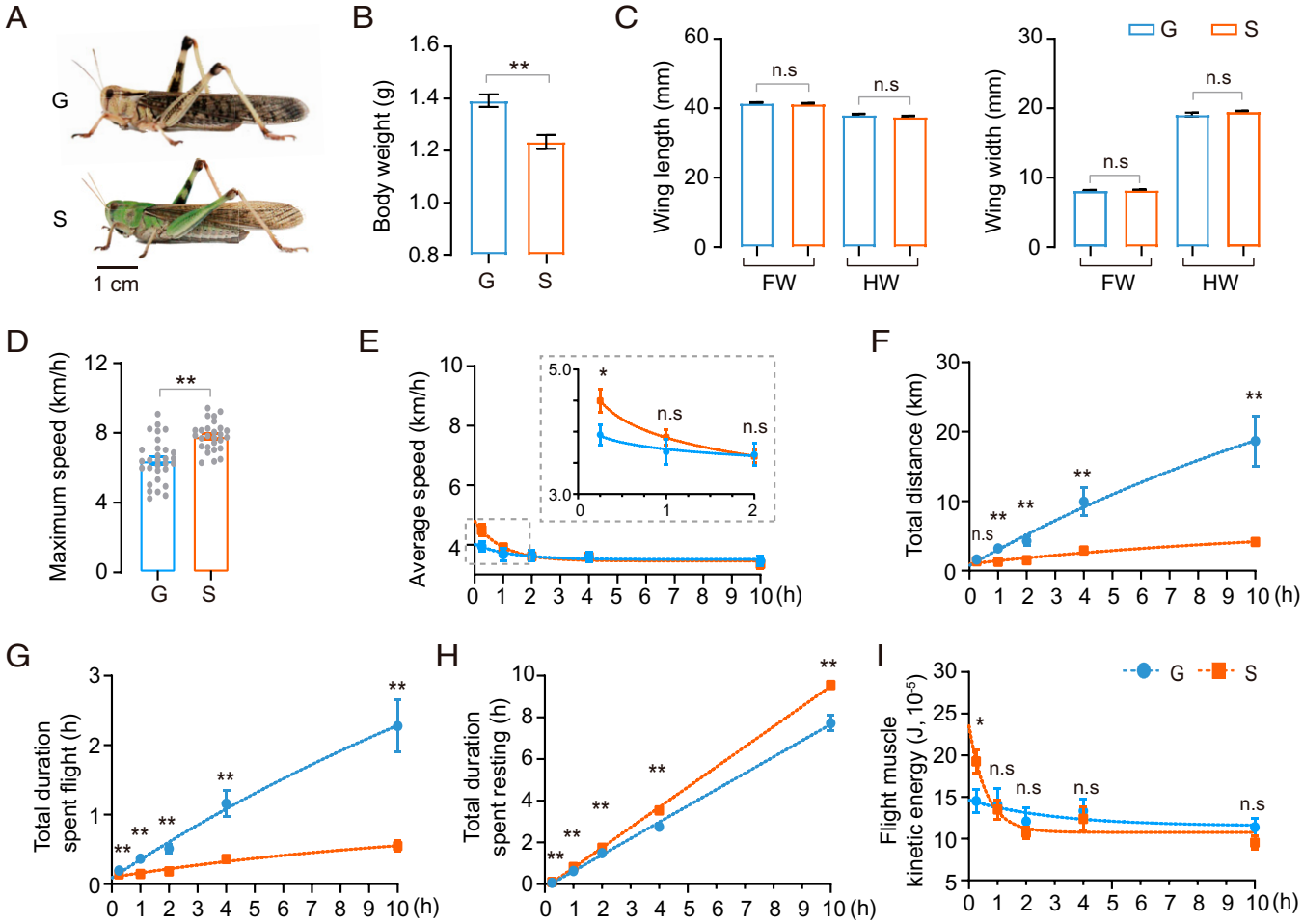

Fig. 1. Flight trait divergence between gregarious and solitary locusts. (*A*) Typical gregarious and solitary adult locusts. G and S represent gregarious and solitary locusts, respectively ($n = 28$ individuals, Student's *t* test). (*B* and *C*) Morphological comparisons between G and S. FW and HW represent forewing and hindwing, respectively ($n \geq 20$ individuals, Student's *t* test). (*D*) Comparison of maximum flight speed between G and S. Each dot represents a single individual (Mann–Whitney *U* test). (*E–H*) The measurement of flight parameters (*E*) average flight speed, (*F*) total flight distance, (*G*) total duration of flight, and (*H*) total duration of resting. (*I*) Comparison of flight muscle kinetic energy between G and S during flight. Flight performance for 0.25-, 1-, 2-, 4-, and 10-h tests were compared. Data for each time point was obtained independently, $n \geq 20$ individuals at each time point (Mann–Whitney *U* test). The fitting curve was obtained by nonlinear regression. All data are presented as the mean ± SEM, $^*P < 0.05$, $^{**}P < 0.01$, and n.s, not significant.

gregarious locusts at all flight-test time points (flight for 0.25 and 1 h; Fig. 2*F* and *SI Appendix*, Fig. S4). Moreover, the enzyme activities of HK, PYK, and CS were also significantly higher in solitary locusts during flight (Fig. 2 *G* and *SI Appendix*, Fig. S5). Therefore, solitary locusts maintained a higher energy metabolism during flight.

As one of the rate-limiting enzymes of the TCA cycle, CS was assumed to be an important control point for metabolic activity determination (29). To verify the effect of energy metabolism on the flight traits of the locusts, the metabolic level was repressed by knocking down *CS*. The injection of double-stranded RNA (dsRNA) of *CS* significantly repressed the gene expression and enzyme activities in flight muscles (Fig. 2*H*). Meanwhile, the knockdown of *CS* significantly repressed the resting CO_2 production rate (Fig. 2*H*), and the initial flight speed (Fig. 2 *I* and *J*), but it had no obvious effect on prolonged flight performance. Therefore, this result suggests that a high Krebs cycle capacity, as observed in solitary locusts, is necessary for the high initial flight speeds that the solitary-phase locusts exhibit.

Rapid Reactive Oxygen Species Accumulation Impairs the Prolonged Flight Ability of Solitary Locusts. To compare metabolic changes with gene expression profiles we tested the metabolite dynamics of solitary and gregarious locusts during flight. Ultrahigh-performance liquid chromatography–high-resolution mass spectrometry was used to compare the relative levels of metabolites after 0, 0.25, and 1 h of flight treatment. The principal component analysis (PCA) revealed that the samples of gregarious and solitary locusts were significantly separated into two categories and the overall metabolite distributions were much more intense in response to flight in solitary locusts than in gregarious ones (Fig. 3*A*). Moreover, 218 and 356 metabolites showed significant differences in response to flight treatments in gregarious and solitary locusts, respectively ($P < 0.05$; *SI Appendix*, Table S1). For all the differential metabolites, the top five metabolite classes were found to be triacylglycerol (TAG), glycerophosphocholine (PC), glycerophosphoethanolamine (PE), amino acid, and carbohydrate (*SI Appendix*, Fig. S6). TAG and carbohydrate decreased during the flight of gregarious and solitary locusts, but TAG dropped more rapidly in solitary locusts than in gregarious ones after 0.25 h of flight (Fig. 3*B* and *SI Appendix*, Fig. S7). Plasmalogen, a class of glycerophospholipids containing a vinyl-ether and an ester bond at the sn-1 and sn-2 positions, was maintained at a higher level in gregarious locusts (Fig. 3*C*).

Metabolic pathway enrichment was subsequently conducted using the overrepresentation method. Fisher's exact test and

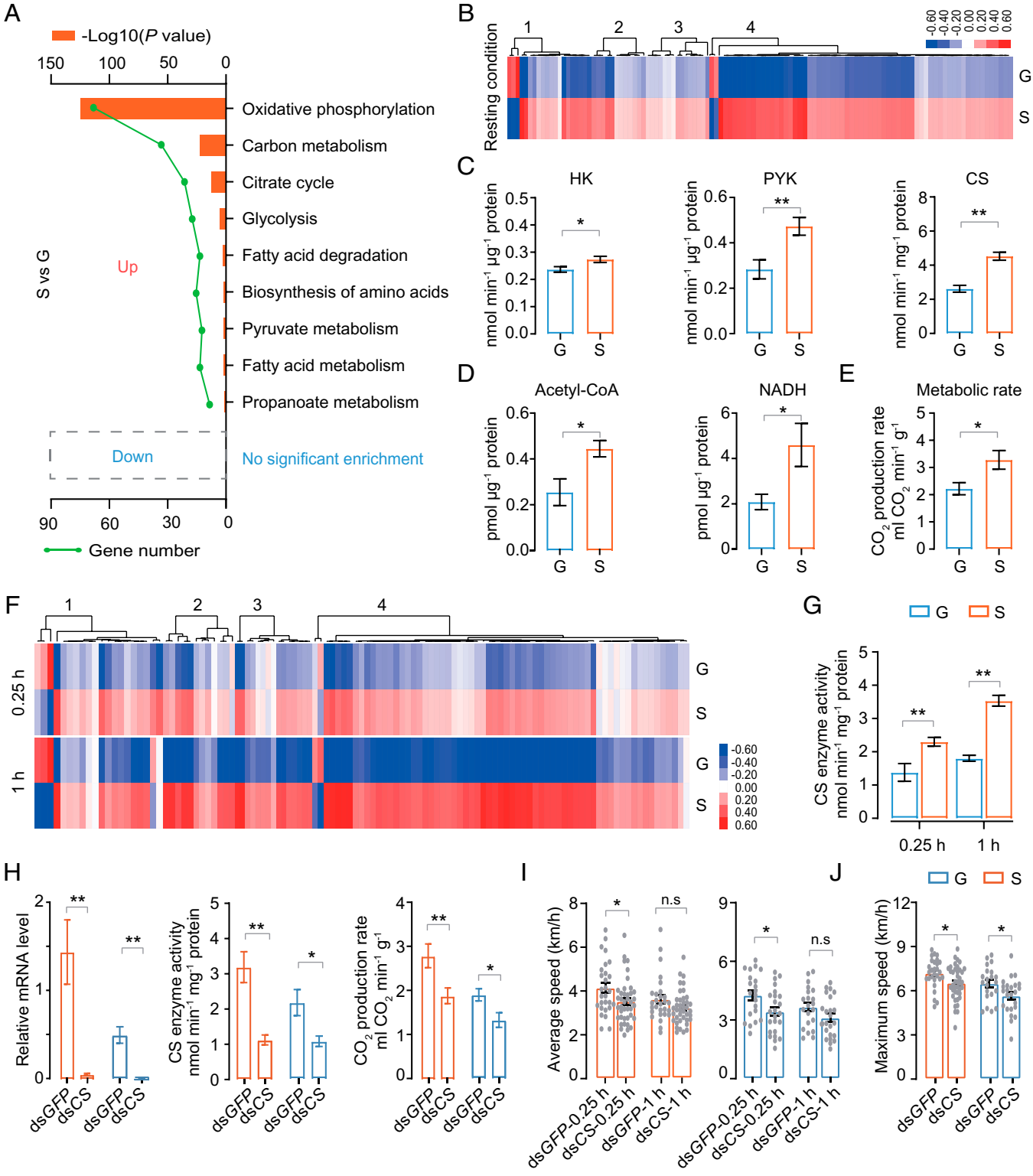

Fig. 2. Energy metabolic profile differences between gregarious and solitary locusts. (*A*) KEGG enrichment of DEGs. Only KEGG terms with adjusted $P < 0.01$ are shown (Fisher's exact test). (*B*) Heat map representing the gene-expression levels is involved in energy metabolism under resting conditions. The four numbers on the top dendrograms represent the different energy metabolism processes, as follows: 1, glycolysis and pyruvate metabolism; 2, fatty acid metabolism; 3, citrate cycle; and 4, oxidative phosphorylation. Heat-map signal indicates $\log_2$ fold-change value relative to the mean expression level within the group. Red signal represents higher expression, whereas blue represents lower expression. (*C*) Enzyme activity of hexokinase (HK), pyruvate kinase (PYK), and citrate synthase (CS) ($n \geq 7$, Student's *t* test). (*D*) Acetyl-CoA and NADH content measurement in the flight muscle of locusts ($n \geq 7$, Student's *t* test). (*E*) MR measurement ($n = 11$, Student's *t* test). (*F*) Heat map representing the expression levels of genes involved in energy metabolism at 0.25- and 1-h postflight treatment. (*G*) Comparison of CS enzyme activity under flight conditions ($n = 7$, Student's *t* test). (*H*) CS knockdown abolished *CS* RNA level and enzyme activity ($n \geq 7$) and decreased CO_2 production rate ($n \geq 11$, Student's *t* test). The levels were examined 72 h after dsRNA injection. (*I* and *J*) Comparison of speed-related flight parameters between controls and *CS*-silencing locusts ($n \geq 20$ individuals, Mann–Whitney *U* test). Each dot represents a single individual. ds*CS* represents CS knockdown. ds*GFP* served as the control. Mean ± SEM. Significant differences are denoted by $^*P < 0.05$, $^{**}P < 0.01$, and n.s, not significant. G and S represent gregarious and solitary locusts, respectively.

out-degree centrality algorithm were used for pathway topology analysis. The metabolites related to butanoate, starch, sucrose, alanine, and glycerophospholipid metabolism exhibited similar change trends between gregarious and solitary locusts after the flight treatment (Fig. 3*D*). In addition to the common pathways that were enriched in both solitary and gregarious locusts, pathways involved in purine metabolism, glutathione metabolism, beta-alanine metabolism, and aminoacyl-transfer RNA biosynthesis were specifically enriched in solitary locusts ($P < 0.05$; Fig. 3*D*). The contents of metabolites involved in purine metabolism (inosinic acid, hypoxanthine, xanthine, and uric acid), and glutathione metabolism, such as reduced glutathione (GSH) and oxidized glutathione (GSSG), changed significantly in solitary locusts in response to the flight treatment. The relative levels of uric acid and GSH in solitary locusts decreased significantly after the 0.25-h flight treatment, and their levels were low until 1 h of flight. By contrast, the levels of uric acid and GSH in the gregarious locusts remained unchanged (Fig. 3 *E* and *F*).

Uric acid and GSH are important antioxidants that rapidly decrease in solitary locusts, but gregarious and solitary locusts showed no significant difference in antioxidant genes expression (*SI Appendix*, Fig. S8). Thus, we speculated about the possibility of rapid reactive oxygen species (ROS) production. When testing the effect of flight on H_2O_2 level in flight muscles, we found that H_2O_2 content dramatically increased in solitary locusts at all time-course points, but no significant increase was found in gregarious locusts after the same flight treatment (Fig. 3*G*).

To explore the effect of oxidative stress on flight performance, we increased oxidative stress by injecting different concentrations of paraquat at a dose range of 0.008 to 0.2 μmol per locust. The contents of H_2O_2 and GSH/GSSG, as well as flight performance, were measured. When the concentration of paraquat was above 0.04 μmol, a significant elevation in H_2O_2 level and reduction in GSH/GSSG level was observed (Fig. 3*H*). Meanwhile, 0.04 μmol of paraquat was sufficient to repress flight distance and duration (Fig. 3*I*). Thus, the limited flight duration of solitary locusts was possibly due to the rapid accumulation of oxidative stress.

Gregarious Locusts Maintain More Energetic Storage. To investigate whether energy storage is a determinant of differential flight traits of gregarious and solitary locusts we measured the contents of lipid and glycogen, both of which are important energy resources in fat bodies. Lipid reserves are stored primarily as TAG in lipid droplets (LDs) (30). The size of LDs from 14-d-old adults was measured through Nile red staining. The relative sizes of LDs were significantly larger (Fig. 4*A*) and TAG content was higher (Fig. 4*B*) in gregarious locusts. However, gregarious and solitary locusts did not significantly differ in glycogen content (Fig. 4*B*). These data confirmed that gregarious locusts had larger TAG storage than solitary ones. When solitary and gregarious locusts were forced to fly for 1 h, which was approximately twofold the average total flight duration of solitary locusts in 10 h of flight tests (Fig. 1*F*), no obvious reduction in TAG content was observed (Fig. 4*C*). Thus, the flight duration and distance of solitary locusts were not restricted by the low energy storage in fat bodies.

Population Density Experiences Establish Basic Energy Metabolism and ROS Generation for Flight Traits. To determine whether flight traits and energy metabolism patterns were density-dependent we performed bioassays on the isolation of gregarious locusts and crowding of solitary locusts. One-day-old adult solitary and gregarious locusts were crowded and isolated for 13 d, respectively. Typical solitary and gregarious locusts were used as controls. The levels of expression of key genes involved in energy metabolism (*COX4*, *ATPsyn*, and *NDUFA*) were measured. Gene expressions of solitary locusts after crowding treatment decreased significantly compared with those of typical solitary locusts. By contrast, the same genes were elevated dramatically during the isolation of gregarious locusts (Fig. 5*A*). In line with the gene-expression profiles, CS activity and CO_2 production rate were reduced in response to crowding treatment and elevated in response to isolation treatment (Fig. 5*B* and *C*). Thus, the characteristics of basic energy metabolism in solitary and gregarious locusts were determined by population density experiences.

The flight performances were compared after isolation and crowding treatments, respectively. After isolation, the short-term flight and maximum flight speeds of gregarious locusts were significantly elevated, but the flight distance and flight duration were reduced in 0.25- and 1-h flight tests, respectively (Fig. 5*D*). By contrast, the crowding of solitary locusts significantly increased their flight distance and flight duration, but their average and maximum flight speed were reduced (Fig. 5*G*). Additionally, flight-induced oxidative stress was tested in response to crowding and isolation treatments. The isolation of gregarious locusts significantly elevated the generation of oxidative stress, which involved the reduction of GSH/GSSG and the elevation of H_2O_2 level after flight treatment (Fig. 5 *E* and *F*). By contrast, the crowding of solitary locusts repressed their H_2O_2 level and elevated their GSH/GSSG level after flight treatment (Fig. 5 *H* and *I*). Therefore, the different flight traits of solitary and gregarious locusts were determined by basic energy metabolic profiles and ROS generation and can be reversed by changing the population density.

Discussion

Our study showed that the flight trait differentiation between solitary and gregarious locusts was primarily attributed to the divergence of energy metabolism, which was determined by different experiences of population density. Robust energy metabolism in flight muscles of solitary locusts facilitated their short-term flight ability and speed. However, their prolonged flight performance was limited because of the overload in oxidative stress. By contrast, gregarious locusts exhibited moderate aerobic activity in their flight muscles, can sustain flight at a relatively low speed, and maintain stable redox homeostasis (Fig. 6).

Environment-dependent flight capacity polyphenism is an adaptive strategy that underpins the ecological success of many insects. This study reported an interesting flight strategy for the migratory locust to cope with changes in population density. The migratory locust can transform from a solitary form to a gregarious one at elevated population density (6). Solitary and gregarious locusts displayed different flight traits, and such differentiation perfectly matched the biological characteristics of the locust phase. In case of food scarcity and absence, long-distance swarm migration occurs in response to unfavorable conditions (31, 32). Thus, the sustained flight ability of gregarious locusts is critical to searching for new food resources or ideal reproductive areas. By contrast, under low-density conditions with adequate food supply, a short sprint ability is sufficient for solitary locusts to avoid predators or to search for mates. Therefore, in addition to a transition in body color and toxic signals (17, 33), flight trait variation is an important feature of locusts. Additionally, crowded conditions reportedly increase the flight performance of wing-monomorphic insects, such as African armyworm, beet webworm, and Oriental armyworm (34–36). Thus, the flight trait variation of insects may be a widespread adaptive strategy for many wing-monomorphic insects.

Gregarious and solitary locusts exhibited differential energy metabolism in their flight muscles. Solitary locusts exhibited

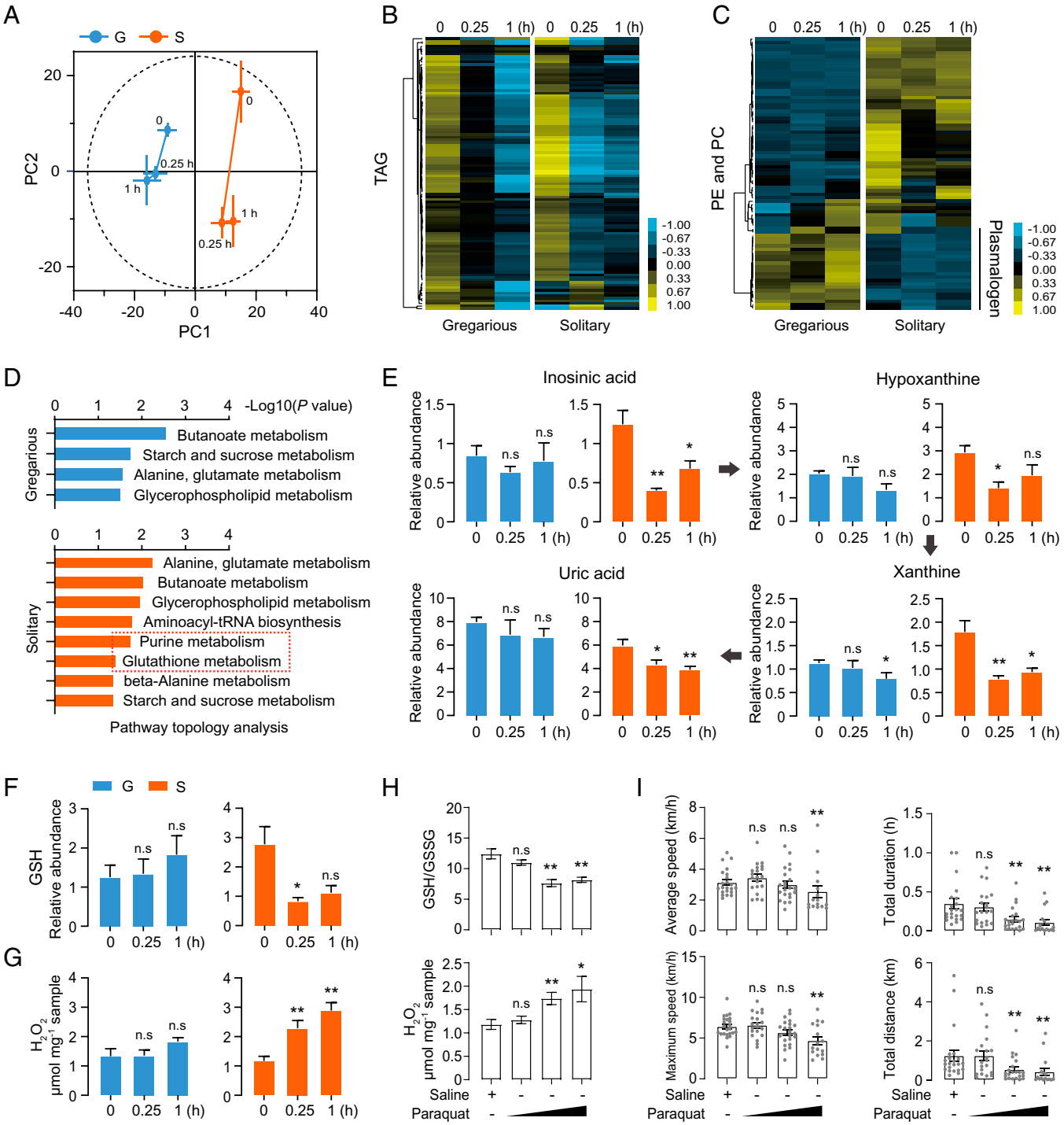

Fig. 3. Metabolome analysis reveals altered oxidative tolerance of solitary and gregarious locusts. (*A*) PCA trajectory analysis of altered metabolites in gregarious locusts (blue point) and solitary locusts (orange point) in response to 0.25 and 1 h of flight treatment. Bar lines indicate SEM of PC1 and PC2. Five biological replicates for each flight treatment time point, and each replicate contains six locusts. Content changes of (*B*) TAG and (*C*) PE and PC during flight. Heat-map signal indicates $\log_2$ fold-change value relative to the median expression level within the gregarious and solitary groups, respectively. Yellow and blue signals represent higher and lower levels, respectively. The dendrograms generated by the hierarchical clustering of metabolites are also provided. TAG: triacylglycerol, PC: glycerophosphocholine; PE: glycerophosphoethanolamine ($n = 5$ replicates, six locusts per replicate). (*D*) Pathway topology analysis of altered metabolites after flight treatment. Only pathways with $P < 0.05$ are shown (Fisher's exact test). (*E*) Content changes in purine intermediate metabolite levels and (*F*) GSH during flight ($n = 5$). (*G*) H_2O_2 alterations in response to flight ($n = 8$). Time points are shown as 0.25- and 1-h flight treatment, each time point is compared to rest condition samples, Student's *t* test. (*H*) GSH/GSSG and H_2O_2 alterations in response to paraquat treatment in the flight muscles ($n \geq 7$, Student's *t* test). (*I*) Flight performance measurement in response to paraquat treatment ($n \geq 17$ individuals, Mann–Whitney *U* test). Each dot represents a single individual. Paraquat (2 μL) was injected at concentrations of 4, 20, and 100 mmol·L^{-1} for 48 h. Locusts injected with saline (2 μL) served as the negative control. Different concentration samples are compared to the negative control. The data are shown as mean ± SEM, $*P < 0.05$, $**P < 0.01$, and n.s, not significant. G and S represent gregarious and solitary locusts, respectively.

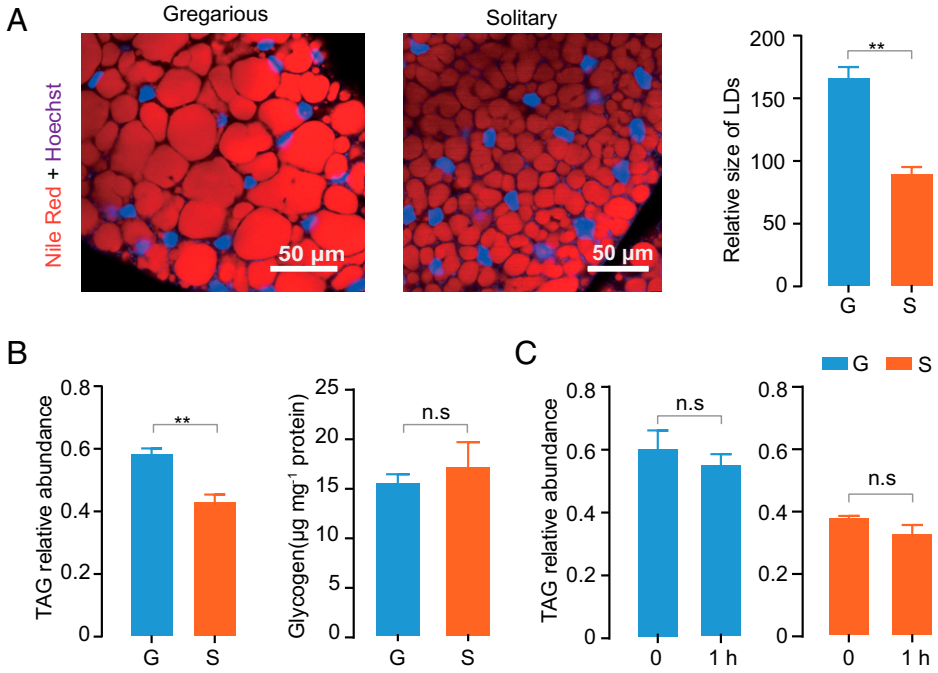

Fig. 4. Levels of TAG and glycogen storage. (*A*) Nile red staining was performed in fat bodies and the relative size of LDs was quantitatively analyzed. (*B*) Relative TAG abundance and glycogen content measurement ($n = 5$, Student's t test). (*C*) TAG content measurement before and after 1 h of forced-flight treatment ($n \geq 5$, Student's t test). G and S represent gregarious and solitary locusts, respectively. The data are shown as mean ± SEM, $^{**}P < 0.01$, and n.s, not significant.

higher mitochondrial energetic storage (Acetyl-CoA and NADH), energy metabolic gene-expression levels, and metabolic enzyme activities in their flight muscles than the gregarious ones. When we repressed the metabolic activity of locusts by knocking down CS expression, their short-term flight speed also decreased. Thus, the high levels of energy metabolism in the flight muscles of solitary locusts allowed high-speed and short-term flight. Flying animals primarily rely on the oxidation of carbohydrates and lipids to fuel their flight (30, 37, 38). In locusts, carbohydrates are typically used at the initial stage of flight or during short-term flight. Conversely, long-term flight requires lipid oxidation (39). The oxidation of carbohydrates in the mitochondria can promote the rapid production of ATP, which can support the high energy requirements of short-term sprint flight (40). However, lipid oxidation can support a substantially lower maximum rate of ATP turnover, indicating that the process can power only the lower energetic requirements of long-term or migratory flight. Thus, at the initial stage of flight or during a short-term flight, the flight speed is determined by carbohydrate consumptive rate and mitochondrial activities.

The lower ROS generation of gregarious locusts facilitates their ability to perform a long-distance flight. In solitary locusts, significantly reduced uric acid and GSH levels and elevated H_2O_2 levels during flight indicated rapid ROS accumulation, which significantly repressed their flight sustainability. Oxidative stress is possibly a key determinant of restricted prolonged flight ability of locusts. Insect flight is a completely aerobic process. Aerobic respiration in the mitochondria is the main source of ROS, and high aerobic performance is always associated with intense ROS generation (41). An overload in ROS production induces oxidative stress and harms cells or tissues by activating a chain reaction of lipid peroxidation. Thus, maintaining a stable redox balance is important for flying adaptation (42). In our study, gregarious locusts during flight maintained a redox balance through low-energy metabolism activity and high plasmalogen content. Moderate metabolic activity can reduce ROS production rate, and a high plasmalogen content can provide other phospholipid and lipoprotein particles protection against oxidative damage (43).

The relationship between energy metabolism activity and the long-distance flight ability of animals is ambiguous. Several metabolic patterns have been observed in flying animals, especially in insects with long-distance flight performance. For example, populations of the cotton bollworm *Helicoverpa armigera*, which has great long-distance flight ability, have high lipid metabolic gene expression levels (24). By contrast, the flight MR is lower in migratory populations of the monarch butterfly than in nonmigratory populations (22, 24). Robust MR and high metabolic gene expression level hardly provide any positive contribution to the long-distance flight of locusts because of excessive oxidative stress accumulation. Thus, a balance between energy supply and oxidative stress is important for the long-distance flight of locusts.

Sufficient energy storage is also important for long-distance flights. Lipids are the major energy resources for prolonged flight and are primarily stored in fat bodies in migratory locusts. In flight, stored TAGs are catalyzed into 1,2-diacylglycerol and transported through the hemolymph into the flight muscles (19). Gregarious locusts have higher TAG storage in fat bodies, whereas solitary ones have a higher AKH content in corpora cardiac but have limited prolonged flight performance (44). This phenomenon is explained by the solitary locusts have less intense hyperlipemia response to flight in hemolymph and require more AKH content to mobilize energy metabolism, which focuses on single prereproductive migratory flight (45, 46). In our study, when solitary locusts were forced to fly constantly for 1 h, which was much longer than their spasmodic bouts of flight (Fig. 1*F*), no obvious reduction in TAG content was observed in fat bodies. Thus, we propose that the short flight duration of solitary locusts is not restricted by relatively low TAG storage in fat bodies. However, oxidative stress, which is a by-product of the higher metabolic profile, restricts the prolonged flight activity of solitary locusts. Less ROS generation and high TAG storage contributes to the long-distance flight of gregarious locusts.

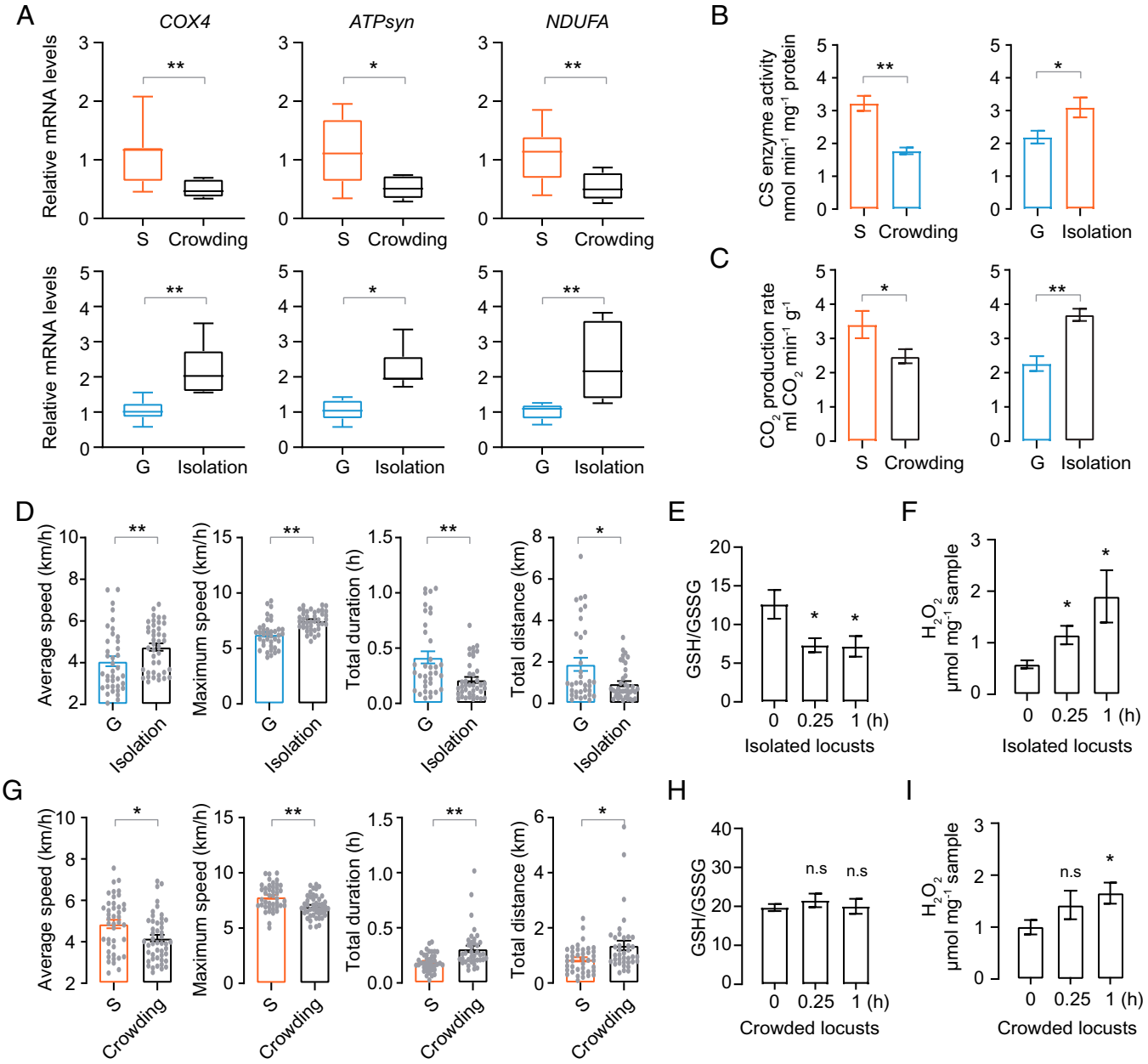

Fig. 5. Energy metabolism and flight trait are reshaped by population density changes. G and S represent gregarious and solitary locusts, respectively. (*A*) Expression profiles of key genes related to aerobic energy metabolism in response to the crowding and isolation treatment, respectively ($n = 8$, Student's t test). (*B*) Citrate synthase enzyme activity measurement ($n = 8$, Student's t test). (*C*) CO_2 production rate measurement ($n = 11$ individuals, Student's t test). Isolation treatments were normalized to typical gregarious locusts, and crowding treatments were normalized to typical solitary locusts. (*D*) Flight performance comparison after isolation treatment ($n \geq 30$ individuals, Mann–Whitney U test). Each dot represents a single individual. (*E* and *F*) GSH/GSSG and H_2O_2 content measurement of isolated locusts during flight ($n \geq 6$, Student's t test). (*G*) Flight performance comparison after crowding treatment ($n \geq 30$ individuals, Mann–Whitney U test). (*H* and *I*) GSH/GSSG and H_2O_2 content measurement of crowded locusts during flight ($n \geq 6$, Student's t test). Time points are shown as 0.25- and 1-h flight treatment, each time point is compared to rest condition samples. The data are shown as mean ± SEM, $*P < 0.05$, $**P < 0.01$, and n.s, not significant.

Population density changes can reverse the metabolic profiles in migratory locusts. Our study indicated that locusts can switch their flight traits and energy metabolism patterns in response to the alteration in population density. Such rapid plasticity explains why locusts possess different phase-related flight traits within one generation. Previous studies found that gregarious nymphs are highly active in behavior and possess a higher CO_2 production rate than solitary nymphs (16, 47). Here, a completely reversed metabolic profile was observed in the flight muscles of adult locusts. These differences in resting MRs between nymphs and adults may be related to factors such as developmental stage or behavior. The density-dependent alterations in metabolism are systematic and possibly regulated by multiple physiological signals and pathways. Therefore, further studies are needed to elucidate the underlying molecular mechanisms.

As the most widely distributed and one of the most notorious locust species, the migratory locust, which has long-distance flight ability, remains a serious threat to food security. The locust adopted a reduced energy metabolism rate strategy to

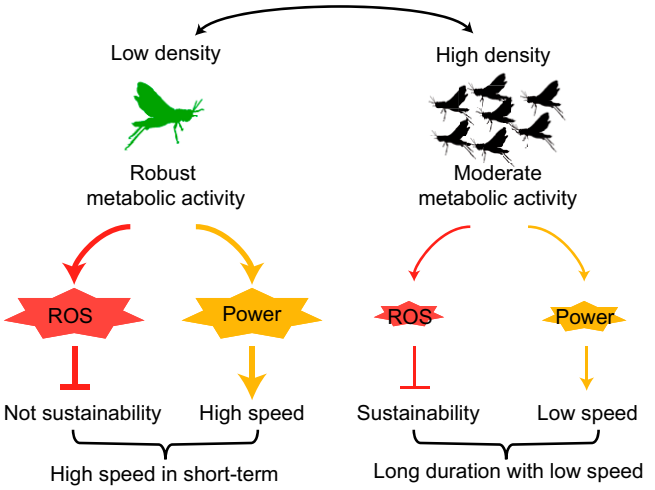

Fig. 6. Mechanism of density-dependent flight trait variation of migratory locusts. At low population density, solitary locusts exhibit robust energy metabolism activity, which produces more power for short-term flight. However, an overload of oxidative stress, which is a by-product of aerobic activity, inhibits their flight sustainability. By contrast, moderate metabolic activity in gregarious locusts maintains a relatively lower ROS generation, thereby facilitating the sustainability of their long-term flight.

acquire less ROS generation for long-distance flight. This finding enhanced our understanding of the relationship between energy metabolism rate and long-distance flight capacity and provides valuable insights into the flight adaptation strategies of flying animals.

Materials and Methods

Insects and Experimental Treatments. Locusts used in this study were from gregarious and solitary locust colonies maintained in the Institute of Zoology, Chinese Academy of Sciences. Gregarious locusts were cultured in large boxes ($40 \times 40 \times 40$ cm^3) at a density of ~300 insects per container for at least eight generations. Solitary locusts were cultured alone in white metal boxes ($10 \times 10 \times 25$ cm^3) supplied with fresh air for at least 10 generations before experiment action. This colony was maintained under a 14-h light:10-h dark photocycle regime at 30 ± 2 °C and fed on fresh wheat seedlings.

One-day-old adults were used for isolation and crowding treatments. For the isolation treatment, gregarious adults that eclosed within 24 h were reared under the solitary condition as described above. For the crowding treatment, the solitary adults that eclosed within 24 h were reared together with adult gregarious locusts in large boxes. The isolated or crowded locusts were dissected or used for the flight performance tests on the 14th day post eclosion.

Tethered Flight Test and Flight Treatment. Flight experiments were conducted at the same time by using computerized tethered flight mills housed at the Institute of Zoology, Chinese Academy of Sciences. In a typical procedure, the flight arm (radius = 12 cm; flight circumference = 75 cm) was made of hard plastic with the vertical axis secured between two magnets. The magnets ensured the negligible friction between the flight arm and corbelled vertical axis. Individual locusts were attached by the tergal side of the mesothorax to the end of the flight-mill arm by using a thin copper wire that fitted into a sleeve suspended from the flight-arm terminal. This setup enabled the insect to fly rotationally in a horizontal plane. An infrared radiation sensor fixed below the flight arm detected a rotational number of turns so that the flight parameters were recorded. The locust flight was induced by a fan placed above the flight mill (if the interval of 30 s no signal is detected, blow for 2 s, at 1.5 m/s wind speed). In the flight traits test, velocities were calculated by dividing distance flown in a flight bout by the duration of that flight bout and then averaged across all flight bouts within the test period. The flight distance was calculated by multiplying the flight arm circumference by the number of laps flown within the test period. The recording of flight parameters and related calculations are performed automatically by a computer. The flight-mill device was positioned in a room under a photoperiod of 14 h light:10 h dark at 28 °C and 5% humidity.

Based on the mass and flight data, we estimated the flight kinetic energy (KE) during flight process as KE = 1/2 × mass × velocity^2 (joules) (28). Flight muscle mass was determined indirectly by cutting the thorax (shorn of legs) and removing trace nonmuscular features such as fats and components of the digestive tract. Then, the thorax was weighed and soaked in 0.5 mol/L NaOH for 24 h. The cuticular residue was weighed after digestion of the muscle tissue (48).

Flight treatment, as distinguished from tethered flight traits test, was used to investigate the differential regulatory mechanisms between gregarious and solitary locusts. For the sample preparation of flight treatment, 14-d-old adult male solitary locusts were forced to sustained flight for the total duration of 0.25 and 1 h, respectively. Gregarious locusts were treated in the same way. Locusts that stopped flying were artificially stimulated to continue flight. The flight data generated by the flight treatment were not included in the analysis of the locust flight traits detection. Flight muscle or fat body was collected immediately after flight treatment and placed in liquid nitrogen for further tests.

Body Weight and Wing Measurement. Body weight was determined by weighing 14-d-old adult male locusts on an electronic balance. Wing length and width were measured. The forewing and hindwing of each locust were carefully removed at the wing base by using forceps and scissors. Using a digital caliper, the forewing length, forewing width, hindwing length, and hindwing width were measured. The wing landmarks used for each measurement were as follows. Forewing length was from the base of the costal vein to the tip of the apical angle (approximately the apical end of the fourth radial branch). Forewing width was from the apical end of the third radial branch to the anal margin (a line approximately parallel to the body). Hindwing length was from the base of the cubital vein to the apical end of the third medial branch, and hindwing width was from the apical end of the subcostal vein to the anal end of the third anal branch.

RNA Sequencing and Data Processing. Total RNA was extracted from flight muscle (at least three samples with six individuals per sample) by using TRIzol reagent (Invitrogen). Complementary DNA libraries were generated using NEBNext UltraTM RNA Library Prep Kit for Illumina (NEB) following the manufacturer's recommendations, and index codes were added to attribute sequences to each sample. Raw data were filtered, and the cleaned data were mapped to the locust genome sequence with HISAT2 software. DEGs were analyzed by using EdgeR software. Additionally, unsupervised hierarchical clustering was performed using Clustal 3.0. RNA-sequencing data were deposited in the Sequence Read Archive Database of NCBI (BioProject PRJNA751147).

qRT-PCR. The relative expression of messenger RNA (mRNA) was quantified with SYBR Green kit (Roche) and LightCycler 480 instrument (Roche). The relative expression levels of specific genes were calculated and quantified using the $2^{-\Delta\Delta Ct}$ method. *Rp*49 was considered as endogenous control for mRNAs. Dissociation curves were determined for each gene to confirm unique amplification. The qPCR primers are listed in *SI Appendix*, Table S2.

Respiratory MR Measurement. Respiratory MR assays were performed as described previously (49). The respiratory MR of the locusts was measured at 28 °C environmental temperatures by using a respirometry system (Sable Systems International). We used respiratory gas exchange by estimating CO_2 production rate as a proxy for MR. The MR of the locust was tested in a closed-circuit system with a volume of 116.7 mL. Each locust was enclosed within a chamber of the circuit that had been placed in an incubator. We have a water-scrubbed device, containing calcium sulfate, to remove the water generated during the measurement. The chamber, water-scrubbed device, and CO_2 analyzer were included in the closed circuit. At the beginning of measurement, the circuit system was open to the air scrubbed of water and CO_2 through a tube at a flow rate of 240 mL/min to stabilize the baseline. The circuit system was then transferred to a closed cycle, and the rate of CO_2 production (VCO_2) in the closed-circuit system was continuously recorded every second for at least 5 min. The output of the CO_2 analyzer was digitized (once per second) and recorded using the ExpeData data analysis software (Sable Systems). For the calculation of MR, we selected the period when locust respiration was stable and estimated the MR by calculating the change of CO_2 volume per unit time. MR was calculated as the CO_2 produced per gram body mass per minute using the equation MR = VCO_2 × volume/body mass, where VCO_2 × volume is the change in volume of CO_2 during the selected test time. The VCO2 is obtained from Expedata software records and expressed as a decimal fraction. The volume was 116.7 mL of the closed circuit. All measurements were conducted from 10 AM to 6 PM, to minimize the effect of circadian rhythms on the locusts.

RNA Interference. The dsRNA of *GFP* and *CS* were prepared using a T7 RiboMAX Express RNAi system (Promega) following the manufacturer's protocol. About 3 $\mu g \cdot \mu L^{-1}$ dsRNA (total = 9 μg) was injected into 11-d-old adult locusts at the second ventral segment of the abdomen. The ds*GFP*-injected group served as the control. After 72 h, the locusts were dissected or used for the flight performance tests. The primers for gene dsRNA synthesis are listed in *SI Appendix*, Table S2.

Enzyme Activity Measurement. CS activity was measured using a Citrate Synthase Activity Colorimetric Assay Kit (Biovision, K318-100) following the manufacturer's protocols. About 10 mg of tissues was homogenized on ice with 100 μL of ice-cold CS assay buffer and centrifuged at 10,000 $\times$ *g* for 5 min. Twenty microliters of supernatant was collected and added into a 96-well plate, and the volume was adjusted to 50 μL with CS buffer. Then, 50 μL of reaction mix was added into each well containing samples, and absorbance (optical density at 412 nm) was measured immediately in kinetic mode at 25 °C for 20 to 40 min. The measured values were normalized to protein levels.

PYK enzyme activity was measured by colorimetric assay using an activity Assay Kit (Solarbio, BC0540) following the manufacturer's protocols. Then, 20 mg of flight muscle tissue of locust was thoroughly homogenized with 400 μL ice-cold extraction buffer. After centrifuging the homogenized tissue at 8,000 $\times$ *g* at 4 °C for 10 min, the supernatant was collected and transferred into a clean tube and kept on ice. The supernatant (20 μL) and reaction buffer (200 μL) were used for the enzyme activity assay. Absorbance was measured at optical density at 340 nm. HK activity was measured with a Hexokinase Assay Kit (Solarbio, BC0745). About 20 mg flight muscle tissue was homogenized with 400 μL ice-cold assay buffer and centrifuged for 10 min at 4 °C at 8,000 $\times$ *g*. Then, 200 μL reaction buffer was added into 10 μL supernatant, and absorbance at optical density at 340 nm was immediately measured in kinetic mode at 25 °C for 5 min. The measured values were normalized to protein levels.

Acetyl-CoA and NADH Measurement. Acetyl-CoA levels were determined using an Acetyl-CoA Assay Kit (Sigma, MAK039-1KT). Fresh muscle tissues were homogenized with 1.0 M perchloric acid. The samples were centrifuged at 10,000 $\times$ *g* for 10 min to remove insoluble material. After concentration, the supernatant was neutralized with 3 M potassium bicarbonate solution. Solution pH was maintained within the range of 6 to 8. Acetyl-CoA levels were measured using a premade reaction mixture following the manufacturer's protocol and then normalized to protein levels.

For NADH measurement, fresh muscle tissue was frozen in liquid nitrogen, homogenized with 400 μL of NADH/NAD extraction buffer, and centrifuged for 10 min at 4 °C at 10,000 $\times$ *g*. Then, the supernatant was centrifuged for 20 min at 4 °C at 10,000 $\times$ *g* by using a 10-kDa spin column (Abcam, ab93349). The filtrate was collected and used for NADH detection with a NAD/NADH Assay Kit (Abcam, ab65348). The measured values were normalized to protein levels.

LD Staining. LDs were visualized by staining fat body tissue with Nile red. Fat body tissues were dissected and washed three times with 1× phosphate-buffered saline (PBS) and incubated for 2 h in Nile red mounting medium (20% [vol/vol] glycerol in PBS, with a 1:10,000 dilution of 10% [vol/vol] Nile red in dimethyl sulfoxide) at room temperature. After two or three washings with 1× PBS, the tissue was incubated for 10 min in Hoechst with 1:500 dilution in PBS and then washed twice with 1× PBS. All images were taken using a Zeiss LSM 710 confocal microscope at 40× magnification with an excitation wavelength of 543 nm and an emission wavelength of 626 nm. The size of LDs was measured using Zeiss ZEN software.

TAG and Glycogen Measurement. Total TAG content was estimated according to previous studies (50). At least three individual tissues were mixed and 0.02 g of sample was homogenized in 100 μL PBS containing 0.5% Tween-20 and incubated at 70 °C for 5 min. Then, all samples were incubated with triglyceride reagent (Sigma, T2449) at 37 °C. After 30 min, the collected supernatant was transferred into 96-well plates after centrifugation and incubated with free glycerol reagent (Sigma, F6428) for 5 min at 37 °C and assayed using SpectraMax Plus384 with a wavelength of 540 nm. TAG amounts were determined by subtracting the amount of free glycerol in the PBS-treated sample from the total glycerol present in the sample treated with triglyceride reagent. TAG levels were normalized to protein levels in each homogenate through BCA assay (Thermo, 23228/23224).

Total glycogen content was determined using a Glycogen Colorimetric/Fluorometric Assay Kit (Biovision, K646–100) according to the manufacturer's protocols. In a typical procedure, 10 mg of muscle tissue was homogenized with 300 μL of double-distilled H_2O and boiled for 10 min. Then, the samples were centrifuged at 14,000 $\times$ *g* for 15 min. The supernatant was reacted with 2 μL of hydrolysis enzyme mix for 30 min at room temperature. Finally, we added 50 μL of reaction mix to each well for 30 min. The measured values were normalized to protein levels in each homogenate.

Metabolomic Profiling. The metabolomic profiling analysis included sample preparation and extraction, metabolite detection, metabolomic data preprocessing, chromatographic peak alignment, and statistical analysis. Details are included in *SI Appendix*.

Paraquat Injection. For paraquat treatment, 12-d-old male adults were selected randomly and separated into four groups (at least 20 individuals per group). Among them, the saline-injected (2 μL per locust) group served as the control for oxidative damage. The remaining three groups were injected with 2 μL of paraquat (Macklin, P814066) at concentrations of 4, 20, and 100 $mmol \cdot L^{-1}$. At 48 h posttreatment, all treated locusts were dissected or used for flight performance tests. The dissected sample tissues were maintained in liquid nitrogen.

Oxidative Stress Measurement. A Hydrogen Peroxide Assay Kit (Beyotime, S0038) was used to determine H_2O_2 content. Flight muscle tissues were harvested and washed with PBS. Ten milligrams of tissue was resuspended in 200 μL of extraction lysis buffer. After homogenization with a vortex shaker, the lysate was centrifuged at 12,000 $\times$ *g* in a microcentrifuge for 5 min at 4 °C. A 50-μL aliquot of supernatant was used for H_2O_2 content determination with 100 μL of detection buffer. Mixed samples were incubated for 30 min at room temperature and assayed using SpectraMax Plus384 with a wavelength of 560 nm. Ratios of reduced to oxidized glutathione (GSH/GSSG) were measured using a GSH/GSSG Ratio Detection Assay Kit (Beyotime, S0053). Ten milligrams of flight muscle tissue was homogenized with 100 μL of assay buffer and centrifuged for 10 min at 4 °C at 10,000 $\times$ *g*. First, total glutathione content was measured. Ten-microliter supernatant samples and 150 μL reaction mix were incubated at room temperature for 5 min. Then 50 μL of the 0.5 mg/mL NADPH solution was added and mixed well. The absorbance at 412 nm was immediately measured in kinetic mode at 25 °C for 25 min. Second, another sample was used for GSSG content measurement. A 50-μL supernatant sample was reacted with 2.5 μL GSH scavenger for 60 min. Then, 10 μL of the solution from the previous step and 150 μL reaction mix were incubated at room temperature for 5 min. Then, 50 μL of the 0.5 mg/mL NADPH solution was added and mixed well. The absorbance at 412 nm was immediately measured in kinetic mode at 25 °C for 25 min. Finally, the amount of GSH is equal to the total glutathione minus GSSG.

Data Availability. RNA-sequencing data have been deposited in the Sequence Read Archive Database of NCBI (BioProject PRJNA751147). All other study data are included in the article and/or *SI Appendix*.

ACKNOWLEDGMENTS. We gratefully acknowledge Jia Yu for the locust sample collection. We also thank Weiguo Du for helpful comments. This study was supported by the National Natural Science Foundation of China (grants 32088102 and 31920103004).

1. H. Chino, P. Y. Lum, E. Nagao, T. Hiraoka, The molecular and metabolic essentials for long-distance flight in insects. *J. Comp. Physiol. B* **162**, 101–106 (1992).
2. K. Iwanaga, S. Tojo, Effects of juvenile-hormone and rearing density on wing dimorphism and oocyte development in the brown planthopper, *Nilaparvata-lugens*. *J. Insect Physiol.* **32**, 585–590 (1986).
3. J. A. Brisson, Aphid wing dimorphisms: Linking environmental and genetic control of trait variation. *Philos. Trans. R. Soc. Lond. B Biol. Sci.* **365**, 605–616 (2010).
4. D. Poniatowski, T. Fartmann, Experimental evidence for density-determined wing dimorphism in two bush-crickets (Ensifera: Tettigoniidae). *Eur. J. Entomol.* **106**, 599–605 (2009).
5. H. J. Xu *et al.*, Two insulin receptors determine alternative wing morphs in planthoppers. *Nature* **519**, 464–467 (2015).
6. N. N. Vellichirammal, P. Gupta, T. A. Hall, J. A. Brisson, Ecdysone signaling underlies the pea aphid transgenerational wing polyphenism. *Proc. Natl. Acad. Sci. U.S.A.* **114**, 1419–1423 (2017).
7. J. Zhao, Y. Zhou, X. Li, W. Cai, H. Hua, Silencing of juvenile hormone epoxide hydrolase gene (Nljheh) enhances short wing formation in a macropterous strain of the brown planthopper, *Nilaparvata lugens*. *J. Insect Physiol.* **102**, 18–26 (2017).
8. C. X. Zhang, J. A. Brisson, H. J. Xu, Molecular mechanisms of wing polymorphism in insects. *Annu. Rev. Entomol.* **64**, 297–314 (2019).
9. M. A. Rankin, J. C. A. Burchsted, The cost of migration in insects. *Annu. Rev. Entomol.* **37**, 533–559 (1992).

10. G. A. Bartholomew, T. M. Casey, Oxygen consumption of moths during rest, preflight warm-up, and flight in relation to body size and wing morphology. *J. Exp. Biol.* **76**, 11–25 (1978).
11. G. Armstrong, W. Mordue, Oxygen consumption of flying locusts. *Physiol. Entomol.* **10**, 353–358 (1985).
12. K. Niitepõld *et al.*, Flight metabolic rate and Pgi genotype influence butterfly dispersal rate in the field. *Ecology* **90**, 2223–2232 (2009).
13. K. Niitepõld, A. L. K. Mattila, P. J. Harrison, I. Hanski, Flight metabolic rate has contrasting effects on dispersal in the two sexes of the Glanville fritillary butterfly. *Oecologia* **165**, 847–854 (2011).
14. M. P. Pener, S. J. Simpson, Locust phase polyphenism: An update. *Adv. Insect Physiol.* **36**, 1–272 (2009).
15. X. Wang, L. Kang, Molecular mechanisms of phase change in locusts. *Annu. Rev. Entomol.* **59**, 225–244 (2014).
16. Z. Ma, W. Guo, X. Guo, X. Wang, L. Kang, Modulation of behavioral phase changes of the migratory locust by the catecholamine metabolic pathway. *Proc. Natl. Acad. Sci. U.S.A.* **108**, 3882–3887 (2011).
17. M. L. Yang *et al.*, A beta-carotene-binding protein carrying a red pigment regulates body-color transition between green am black in locusts. *eLife* **8**, e41362 (2019).
18. W. Guo *et al.*, CSP and takeout genes modulate the switch between attraction and repulsion during behavioral phase change in the migratory locust. *PLoS Genet.* **7**, e1001291 (2011).
19. D. J. Van der Horst, K. W. Rodenburg, Locust flight activity as a model for hormonal regulation of lipid mobilization and transport. *J. Insect Physiol.* **56**, 844–853 (2010).
20. A. Ayali, M. P. Pener, The relations of adipokinetic response and body lipid-content in locusts (*Locusta-migratoria* migratorioides) with special reference to phase polymorphism. *J. Insect Physiol.* **41**, 85–89 (1995).
21. A. Ayali, M. P. Pener, J. Girardie, Comparative study of neuropeptides from the corpora cardiaca of solitary and gregarious *Locusta*. *Arch. Insect Biochem. Physiol.* **31**, 439–450 (1996).
22. S. Zhan *et al.*, The genetics of monarch butterfly migration and warning colouration. *Nature* **514**, 317–321 (2014).
23. V. Talla *et al.*, Genomic evidence for gene flow between monarchs with divergent migratory phenotypes and flight performance. *Mol. Ecol.* **29**, 2567–2582 (2020).
24. C. M. Jones *et al.*, Genomewide transcriptional signatures of migratory flight activity in a globally invasive insect pest. *Mol. Ecol.* **24**, 4901–4911 (2015).
25. X. Wang *et al.*, The locust genome provides insight into swarm formation and long-distance flight. *Nat. Commun.* **5**, 2957 (2014).
26. A. Ryabova *et al.*, Combined metabolome and transcriptome analysis reveals key components of complete desiccation tolerance in an anhydrobiotic insect. *Proc. Natl. Acad. Sci. U.S.A.* **117**, 19209–19220 (2020).
27. S. Guo *et al.*, Aging features of the migratory locust at physiological and transcriptional levels. *BMC Genomics* **22**, 257 (2021).
28. H. Schroeder, A. Majewska, S. Altizer, Monarch butterflies reared under autumn-like conditions have more efficient flight and lower post-flight metabolism. *Ecol. Entomol.* **45**, 562–572 (2020).
29. L. Shi, B. P. Tu, Acetyl-CoA and the regulation of metabolism: Mechanisms and consequences. *Curr. Opin. Cell Biol.* **33**, 125–131 (2015).
30. E. L. Arrese, J. L. Soulages, Insect fat body: Energy, metabolism, and regulation. *Annu. Rev. Entomol.* **55**, 207–225 (2010).
31. J. W. Chapman, D. R. Reynolds, K. Wilson, Long-range seasonal migration in insects: Mechanisms, evolutionary drivers and ecological consequences. *Ecol. Lett.* **18**, 287–302 (2015).
32. S. W. Applebaum, Y. Heifetz, Density-dependent physiological phase in insects. *Annu. Rev. Entomol.* **44**, 317–341 (1999).
33. J. Wei *et al.*, Phenylacetonitrile in locusts facilitates an antipredator defense by acting as an olfactory aposematic signal and cyanide precursor. *Sci. Adv.* **5**, eaav5495 (2019).
34. K. P. Woodrow, A. G. Gatehouse, D. A. Davies, The effect of larval phase on flight performance of African armyworm moths, *Spodoptera exempta* (walker) (Lepidoptera, Noctuidae). *Bull. Entomol. Res.* **77**, 113–122 (1987).
35. H. Kong, L. Luo, X. Jiang, L. Zhang, Effects of larval density on flight potential of the beet webworm, *Loxostege sticticalis* (Lepidoptera: Pyralidae). *Environ. Entomol.* **39**, 1579–1585 (2010).
36. X. Jiang, L. Luo, L. Zhang, T. W. Sappington, Y. Hu, Regulation of migration in *Mythimna separata* (Walker) in China: A review integrating environmental, physiological, hormonal, genetic, and molecular factors. *Environ. Entomol.* **40**, 516–533 (2011).
37. R. K. Suarez *et al.*, Fuel selection in rufous hummingbirds: Ecological implications of metabolic biochemistry. *Proc. Natl. Acad. Sci. U.S.A.* **87**, 9207–9210 (1990).
38. R. K. Suarez *et al.*, Energy metabolism in orchid bee flight muscles: Carbohydrate fuels all. *J. Exp. Biol.* **208**, 3573–3579 (2005).
39. H. J. Pflüger, C. Duch, Dynamic neural control of insect muscle metabolism related to motor behavior. *Physiology (Bethesda)* **26**, 293–303 (2011).
40. D. J. Van der Horst, N. M. D. Houben, A. M. T. Beenakkers, Dynamics of energy substrates in the haemolymph of *Locusta migratoria* during flight. *J. Insect Physiol.* **26**, 441–448 (1980).
41. D. B. Zorov, M. Juhaszova, S. J. Sollott, Mitochondrial reactive oxygen species (ROS) and ROS-induced ROS release. *Physiol. Rev.* **94**, 909–950 (2014).
42. E. Levin, G. Lopez-Martinez, B. Fane, G. Davidowitz, Hawkmoths use nectar sugar to reduce oxidative damage from flight. *Science* **355**, 733–735 (2017).
43. J. M. Dean, I. J. Lodhi, Structural and functional roles of ether lipids. *Protein Cell* **9**, 196–206 (2018).
44. A. Ayali, M. P. Pener, S. M. Sowa, L. L. Keeley, Adipokinetic hormone content of the corpora cardiaca in gregarious and solitary migratory locusts. *Physiol. Entomol.* **21**, 167–172 (1996).
45. A. Ayali, E. Golenser, M. P. Pener, Flight fuel related differences between solitary and gregarious locusts (*Locusta migratoria* migratorioides). *Physiol. Entomol.* **21**, 1–6 (1996).
46. A. Ayali, M. P. Pener, Density-dependent phase polymorphism affects response to adipokinetic hormone in *Locusta*. *Comp. Biochem. Physiol. A Comp. Physiol.* **101**, 549–552 (1992).
47. Y. Heifetz, S. W. Applebaum, Density-dependent physiological phase in a non-migratory grasshopper *Aiolopus thalassinus*. *Entomol. Exp. Appl.* **77**, 251–262 (1995).
48. S. P. Roberts, J. F. Harrison, R. Dudley, Allometry of kinematics and energetics in carpenter bees (*Xylocopa varipuncta*) hovering in variable-density gases. *J. Exp. Biol.* **207**, 993–1004 (2004).
49. B. J. Sun *et al.*, Phenology and the physiological niche are co-adapted in a desert-dwelling lizard. *Funct. Ecol.* **32**, 2520–2530 (2018).
50. X. Wang *et al.*, Hormone and receptor interplay in the regulation of mosquito lipid metabolism. *Proc. Natl. Acad. Sci. U.S.A.* **114**, E2709–E2718 (2017).